THERMAL MODELING OF PERMANENT MAGNET SYNCHRONOUS MOTOR AND INVERTER

A Thesis
Presented to
The Academic Faculty

by

Mihir N. Rajput

In Partial Fulfillment
of the Requirements for the Degree
Master of Science in the
School of Electrical and Computer Engineering

Georgia Institute of Technology
May 2016

THERMAL MODELING OF PERMANENT MAGNET SYNCHRONOUS MOTOR AND INVERTER

Approved by:

Professor David Taylor, Advisor
School of Electrical and Computer Engineering
Georgia Institute of Technology

Professor Thomas Habetler
School of Electrical and Computer Engineering
Georgia Institute of Technology

Professor Thomas Fuller
School of Chemical and Biomolecular Engineering
Georgia Institute of Technology

Date Approved: 29 April 2016

This thesis is dedicated to my family. My dad, Narendrasingh Rajput, my mom, Nanda Rajput, my brother, Nalin Rajput and the rest of my family in India. I also dedicate this thesis to Georgia Tech's EcoCAR-3 team.

ACKNOWLEDGEMENTS

This is the most fun part of the thesis. First, big thanks to my advisor Professor David Taylor. I have learned a great deal from him and I admire his ability to reason on first principles. I also learned from him how to make clever assumptions based on the underlying physical principles and available information. I also want to thank him for keeping me on track whenever I got lost in heaps of information.

I also want to thank Professor Thomas Habetler for teaching me Electric Machine Drives and culminating my interest in that technical area.

My big thanks to EcoCAR-3 teammates especially Dr. Fuller for advising us on HV safety. Special thanks to Parker and SEVCON for sharing data with Dr. Taylor and myself without which this wouldn't have been possible.

Finally I want to thank the best mom and dad in the world for their constant support throughout. I also want to thank my brother and my school friends for constant encouragement.

TABLE OF CONTENTS

LIST OF TABLES

LIST OF FIGURES

SUMMARY

The purpose of my thesis is to establish a simple thermal model for a Parker GVM 210-150P motor and a SEVCON Gen4 Size8 inverter. These models give temperature variations of critical components in the motor and the inverter. My thesis will help Georgia Tech's EcoCAR-3 team in understanding the physics behind thermal modeling and why thermal study is necessary. This work is a prerequisite for Software in the Loop (SIL) simulations or Hardware in the Loop (HIL) simulations for a hybrid electric vehicle.

CHAPTER I

INTRODUCTION

1.1 Overview

EcoCAR-3 is the most recent of the US Department of Energy's Advanced Vehicle Technology Competition series. The objective of this competition is to redesign a Chevrolet Camaro as a hybrid electric vehicle to reduce its environmental impact while maintaining the performance expected from this car. We are also tasked with retaining safety and protection, and high consumer standards of the Camaro. We will be using an electric motor, an inverter and an energy storage system in conjunction with the traditional powertrain.

A torque request will be generated by the vehicle's supervisory controller in response to accelerator and brake pedal positions. Our inverter will operate in torque mode so that the motor output torque matches the commanded value. To ensure maximum performance of the inverter and the motor, we as users of these products have to strictly observe the electrical, mechanical and thermal limits. It is apparent that failures can be prevented by avoiding stressful operation. The purpose of my thesis is to estimate the losses in a motor and an inverter that are fed into thermal models for computing critical average temperature rises. Temperatures must not be allowed to exceed limits to avoid failures. Figure 1 outlines the basic approach employed in this thesis.

1.2 Thesis Organization

Chapter 2 gives an overview of the physical system. This chapter explains in detail the three modes of heat transfer, analogies between voltage and temperature, and

analogies between current and heat flow. Chapter 2 also gives an interpretation of thermal resistances and thermal capacitances. Finally, it highlights a simple yet effective procedure for thermal modeling.

Chapter 3 explains in detail the proposed motor thermal model, elaborating on every component of the thermal network, i.e. independent heat flow source (losses), independent temperature source (reference), thermal resistance and thermal capacitance. This chapter ends with a section on thermal model verification where operating conditions from the datasheet are reproduced using the proposed model to check its accuracy.

Chapter 4 explains in detail the proposed inverter thermal model, elaborating on every component of the thermal network. This chapter ends with a section on thermal model verification where operating conditions from the datasheet are reproduced using the proposed model to check its accuracy.

The thesis concludes with Chapter 5 which discusses inferences made from the proposed motor and inverter thermal model. This chapter also proposes future work. Finally, Appendix A describes the relationship between torque, speed and current and Appendix B contains listings of the MATLAB codes for simulation purposes.

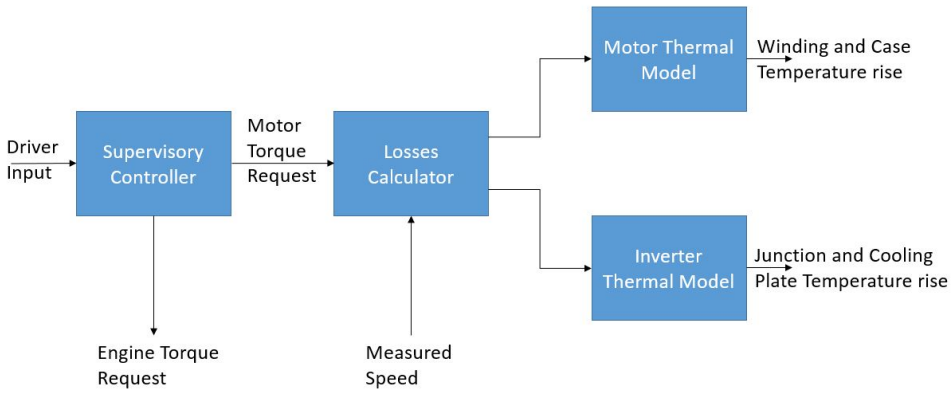

Figure 1: Overview of the thermal modeling system.

CHAPTER II

PHYSICS OF HEAT TRANSFER AND THERMAL MODELING

2.1 Physical System

Our EcoCAR-3 team is using the physical arrangement shown in Figure 2 for cooling the Motor Generator Unit (MGU). We have a separate cooling arrangement for every component of the MGU. However, the cooling system for the inverter and the energy storage system (ESS) share a reservoir. The cooling requirements of the components of the MGU are mentioned in Table 1.

The objective of this chapter is to summarize and explain the physics behind thermal modeling and heat transfer from popular textbooks [1] and [3].

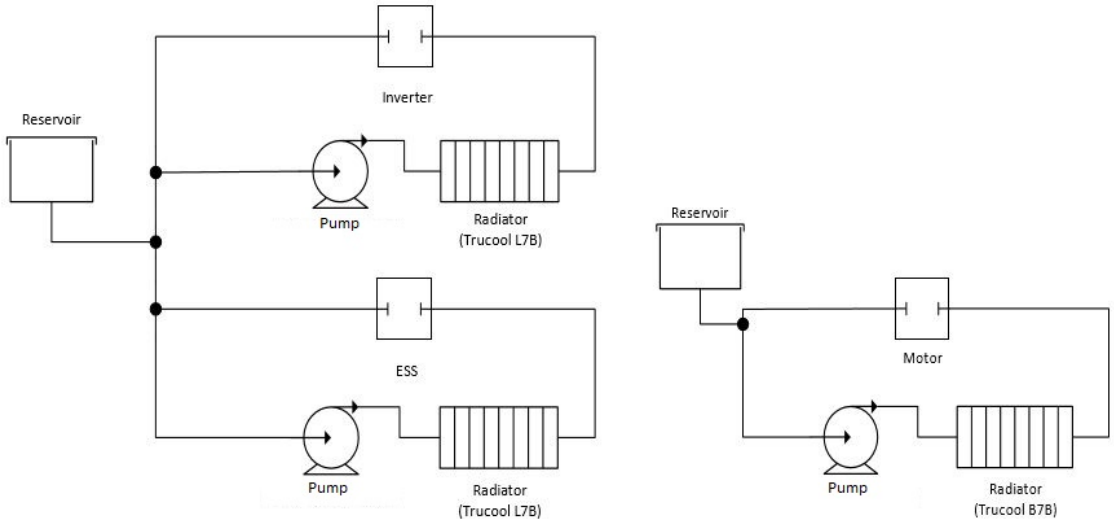

Figure 2: Physical cooling system schematic adapted from [2].

Table 1: Component Cooling Information adapted from [2]

Component	Temperature Requirements	Coolant Type	Flow Rate	Pressure Drop
Motor	Max winding temperature 180 °C	50/50 water and ethylene glycol	5 L/min	70 kPa
Inverter	Max junction temperature 155 °C	50/50 water and ethylene glycol	5 L/min	67 kPa

2.1.1 System Components

2.1.1.1 Pump

A centrifugal pump converts input power to kinetic energy by accelerating liquid in a revolving device - an impeller. The fluid accelerates radially outward and a vacuum is created at the impeller's eye that continuously draws more fluid into the pump. The energy from the pump's prime mover is transferred to kinetic energy. The kinetic energy of a liquid coming out of an impeller is converted to pressure energy by the pump casing.

2.1.1.2 Radiator

Radiators are heat exchangers used to transfer thermal energy from one medium to another for the purpose of cooling and heating. The majority of radiators are constructed to function in automobiles, buildings, and electronics. The radiator is always a source of heat to its environment. In hybrid electric vehicles, the radiators will be used to cool the coolant which takes heat from the engine, motor, inverter and ESS.

2.1.1.3 Motor

An electric motor is a machine that converts input electrical energy to mechanical energy and vice versa. Our team has selected a permanent magnet synchronous motor. We will discuss the motor in detail in Chapter 3.

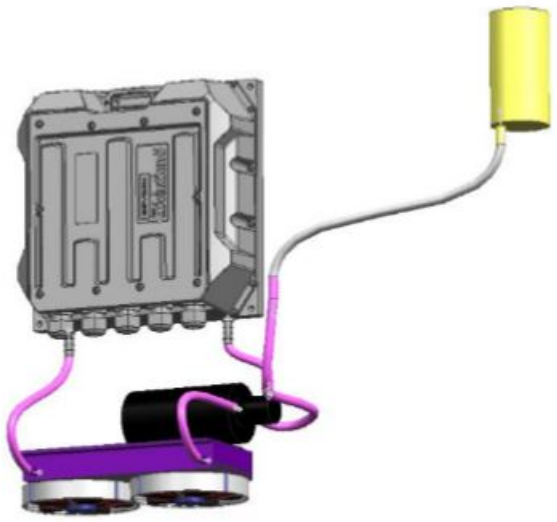

Figure 3: Inverter cooling system adapted from [2].

2.1.1.4 Inverter

An inverter is a device which converts DC power to AC power and vice versa. Since we want to run an AC electric motor, we need an inverter to convert DC supply from the battery to controllable AC supply for the motor. We will discuss the inverter in detail in Chapter 4.

2.1.2 Motor and Inverter Cooling System

Figure 3 and Figure 4 show the inverter and motor cooling system respectively. The reservoir is the highest point in the cooling loop. The radiator, fan and pump are placed below the motor and the inverter.

2.2 Thermal System

A block diagram of a thermal system is shown in Figure 5. A thermal network is an arrangement of thermal resistances and thermal capacitances. By keeping track of the heat generated, we can predict the temperature behavior of various nodes in the thermal network. Subsection 2.2.1 explains the thermal components in detail.

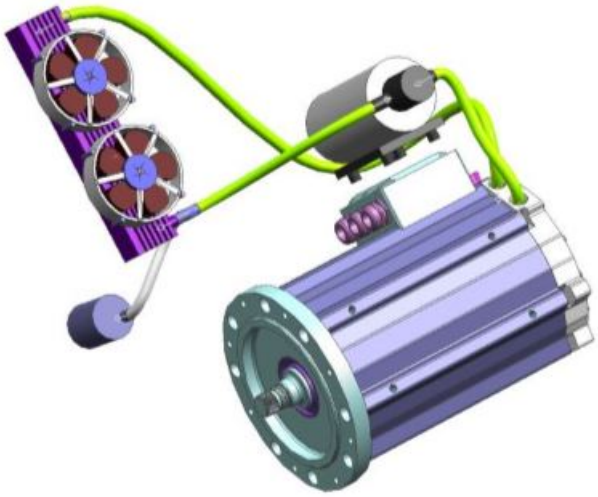

Figure 4: Motor cooling system adapted from [2].

2.2.1 Thermal Variables

2.2.1.1 Temperature

The temperature of an object is a measure of mean kinetic energy of molecules of that object. Since a molecule cannot have negative kinetic energy, absolute temperature of an object cannot be negative. SI unit of temperature is kelvin (K). Temperature at a node in a system is represented by θ_i. Temperature is a potential and it obeys

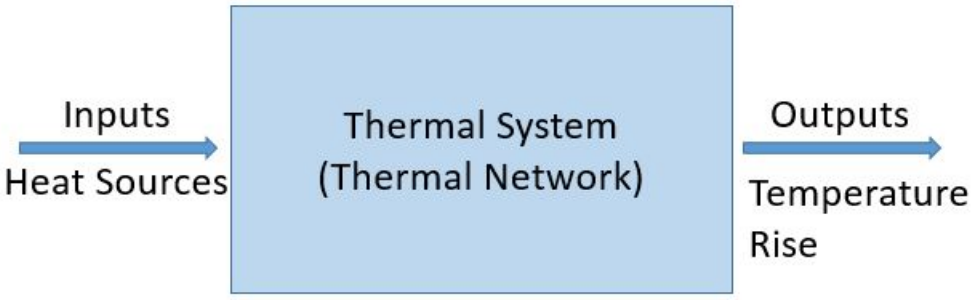

Figure 5: Thermal system.

the path law given by

$$\sum_{loop} A_{ij} = \sum_{loop} A_i - A_j = 0 \tag{1}$$

where A_i is the potential and A_{ij} is the potential difference. Path law implies that potential differences A_{ij} between nodes i and j can be found by adding potential drops across branches along any path from node i to node j i.e. A_{ij} is independent of the path. Kirchoff's voltage law is the path law in electrical domain.

2.2.1.2 Heat Flow

If two objects of different temperatures are brought in contact with each other, temperature of the hotter object decreases and of the cooler object increases. These changes in temperature are explained by a transfer of heat energy from a hotter object to a cooler object. Quantity of heat in an object is represented by H. Therefore, $q \equiv \frac{\mathrm{d}H}{\mathrm{d}t}$, denotes rate of heat flow into the object. Heat flow obeys the node law i.e. sum of flows directed into a node is zero; i.e., energy is conserved. Node law is defined by (2). Kirchoff's current law is the node law in electrical domain:

$$\sum_{node} \theta_i = 0 \tag{2}$$

Node law can be easily inferred from the first law of thermodynamics. Equivalent statements of the first law of thermodynamics are listed below:

1. Energy can neither be created nor can it be destroyed.

2. Increase in amount of energy stored in a control volume must equal amount of energy that enters the control volume, minus the amount of energy that leaves control volume.

3. Rate of increase of thermal and mechanical energy stored in a control volume must equal the rate at which thermal and mechanical energy enters the control

volume, minus the rate at which thermal and mechanical energy leaves the control volume, plus the rate at which thermal and mechanical energy is generated within the control volume.

Only in case of conduction and convection the flow of heat between two points in a system proportional to the temperature difference between the points in the same way that electric current is related to voltage difference. The fundamental difference being, heat flow q is a flow of thermal power; as H itself is the thermal energy. Amount of heat H delivered to an object is positive if it causes temperature of an object to rise. SI unit of heat H is joule (J). While the SI unit of heat flow rate q is watt (W).

2.2.2 Modes of Heat Transfer

Heat transfer is defined as thermal energy in transit due to spatial temperature difference. There are three modes of heat transfer. Each mode has been explained in detail in this subsection.

2.2.2.1 Conduction

Whenever there is a temperature gradient in a stationary medium, solid or a fluid, heat transfer occurs via conduction. At the microscopic level, heat energy is transferred through random molecular motion or diffusion and is enhanced by collisions. The conduction phenomenon is accurately described by Fourier's law, which says, conducted heat flux (heat flow per unit area) is oriented in the direction of greatest rate of decrease of temperature and is proportional to the rate of decrease. Fourier's law is given by

$$q = -kA\frac{\partial\theta}{\partial x} \tag{3}$$

where A is the isothermal surface area perpendicular to direction of heat flow (m^2); k is the transport property "thermal conductivity" (W/mK) and is characteristic of

the conduction medium; and q is the heat transfer rate in watts (W).

2.2.2.2 Convection

Convection refers to the heat transfer that will occur between a surface and moving fluid when they are at different temperatures. Energy transfer occurs through diffusion and bulk motion of the fluid. Transfer of heat from a hot object to a cooler object by circulation of fluid is convection. Regardless of the nature of convection heat transfer process, the appropriate rate equation is given by Newton's law of cooling

$$q = hA(\theta_s - \theta_\infty) \tag{4}$$

where A is the isothermal surface area perpendicular to the direction of heat flow (m^2); θ_s is the surface temperature (K); θ_∞ is the fluid temperature (K); h is the convective heat transfer coefficient (W/m^2K) and depends on surface geometry, nature of fluid motion, fluid thermodynamics and transport properties; and q is the heat transfer rate in watts (W).

2.2.2.3 Radiation

Thermal radiation is the energy emitted by matter that is at a non zero temperature in form of electromagnetic waves. Radiation does not require a material medium. In fact it is most efficient in vacuum. According to the Stefan Boltzmann law, the power emitted by a real body is given by $q = \epsilon\sigma A\theta_s^4$, where θ_s is the absolute temperature of surface (K); A is the isothermal surface area perpendicular to direction of heat flow; σ is the Stefan-Boltzmann constant with a value of 5.67×10^{-8} W/m^2K^4 and dimensionless ϵ is the emissivity of the body. Net energy transfer from a hot body to the environment through radiation is given by

$$q = \epsilon\sigma A(\theta_s^4 - \theta_{sur}^4) \tag{5}$$

where θ_{sur} is the absolute temperature of surrounding (K). Because σ is very small, only large temperature differences will contribute to significant amount of energy

transfer. Typically, for our vehicle, the temperature differences are going to be in the order of 140 K. Hence we can safely neglect heat transfer via radiation. However, in many applications radiation could turn out to be more important than common belief.

2.2.3 Thermal Resistance

Similar to Ohm's law for electrical systems, we have $\theta_{ij} = R_{th}q$ for thermal systems. Experimentally, it has been shown that heat is conducted from an isotherm at temperature θ_i to another isotherm at temperature θ_j, the rate is proportional to the temperature difference $\theta_i - \theta_j$ or θ_{ij} and $\theta_i > \theta_j$. Here the proportionality factor R_{th} is the thermal resistance of an object between the isotherms. R_{th} is an impedance; i.e., a ratio of temperature difference (potential) to heat transfer rate (flow). An ideal thermal resistor is defined as lumped element that obeys linear temperature flow relation. Thermal resistances are used to represent all three transfer phenomenon.

2.2.4 Thermal Capacitance

The ability of an object to store heat is indicated by its specific heat capacity, c_p, which is the amount of heat needed to increase the temperature of 1 g of substance by 1 °C. Consider a homogeneous object at temperature θ_i and mass m. If temperature of the object is raised by $\delta\theta_i$, the heat stored in the object increases by $\delta H = mc_p\delta\theta_i$. Heat transferred to the body is given by

$$q = mc_p\dot{\theta}_i \tag{6}$$

We can substitute temperature difference θ_{io} in (6) if θ_o is constant reference temperature. Then we can express (6) in terms of an impedance

$$\theta_{io} = (1/sC_{th})q \tag{7}$$

where s is the Laplace operator and C_{th} is the thermal capacitance of an object given by $C_{th} = mc_p$. According to (6), we can continue removing heat from an object

as long as we lower its temperature. Since we can't reduce the temperature below absolute zero, we view absolute temperature as the absolute amount of heat stored in an object. Hence $mc_p\theta_{io}$ is amount of heat necessary to raise temperature of an object from θ_o to θ_i. This derivation is based on an important assumption that there is no thermal gradient in the object.

2.2.5 Thermal Sources

2.2.5.1 Ideal Independent Temperature Source

An ideal independent temperature source maintains a specified temperature difference θ_{io} relative to the reference node, regardless of the thermal system connected across its terminals. One terminal of the temperature source is always the reference node. It is similar to the idea of an ideal voltage source which maintains constant potential difference irrespective of the current drawn. However, the difference lies in the power drawn: for an electrical system power is VI but for a thermal system the power drawn is q.

2.2.5.2 Ideal Independent Heat Flow Source

An ideal independent heat flow source maintains a specified heat flow q from the reference node to node i, regardless of the thermal system connected to node i. It is similar to the idea of an ideal current source which maintains a constant current flow.

2.2.6 Lumping Procedure for Thermal Systems

1. Draw a pictorial diagram.

2. Identify isothermal surfaces of significant interest. One of these nodes must be reference node which is usually at ambient temperature.

3. Insert lumped thermal resistors between nodes that are connected by objects with significant thermal conductance.

4. Attach lumped thermal capacitors to the nodes representing objects of high thermal mass and/or high specific heat. Thermal capacitors must be connected to reference node, which need not be isolated at a single location.

5. Insert ideal thermal sources between appropriate nodes and reference node.

6. Draw a thermal circuit. Treat all points connected by solid lines as a single node.

7. Solve the thermal network.

CHAPTER III

MOTOR THERMAL MODELING

3.1 Introduction

A Permanent Magnet Synchronous Motor (PMSM) with high power density and high operating efficiency designed with rare earth based magnets is an attractive choice for hybrid electric vehicle. We have selected and purchased Parker's GVM 210-150P for our application. Predicting the temperature of the motor is of interest to our team for several reasons. Motor failure can result in the failure of the entire system with severe economic consequences, even threat to personal safety; i.e., injury or death. Motors must be operated within the manufacturer specified temperature range to minimize the risk of demagnetization of permanent magnets and/or failure of stator winding. Consequently, the primary goal of developing a motor thermal model is to enable simulation of the system including temperature variation.

Beyond simulation, another motivation for thermal modeling would be online temperature estimation. The Parker motor comes with switch type and linear type temperature sensors built into the stator winding. Temperature estimation software would provide protection in the event that the built in sensors fail. Avoidance of excessive winding temperatures is essential since, as pointed out in [11], 27% of motor failures are due to compromised insulation integrity.

As discussed in Chapter 2, a thermal model of a motor will consist of a lumped-parameter thermal network of thermal resistances and capacitances. This thermal network will be fed from heat flow sources to be described in the following section.

3.2 Loss Modeling

Losses determine the heating of an electric machine. The principal sources of heat will be copper losses, iron losses and friction losses. These are discussed in detail below.

3.2.1 Dissipation Mechanisms

3.2.1.1 Copper Losses

Copper losses P_r are losses caused by resistance of the stator windings. The power dissipated is given by

$$P_r = R(\theta_{m1})(i_d^2 + i_q^2) \tag{8}$$

where $R(\theta_{m1})$ is the per phase resistance of the motor windings at temperature θ_{m1}, and i_d and i_q are components of currents flowing through these winding as described in Appendix A.

3.2.1.2 Iron Losses

Iron losses occur within the magnetic material of a magnetic circuit. They have two components: eddy current losses and hysteresis losses. The first empirical equation to govern iron power losses, proposed by Dr. Steinmetz in 1892, is $P = k_1 \hat{B}^\beta$, where $\hat{B}$ is the peak flux density, k_1 and β are statistically fitted coefficients to experimental data.

Eddy Current Losses According to Faraday's law of electromagnetic induction, closed path emfs are induced in the stator core because of the rotating magnetic field in the motor. According to Ampere's law, these currents will flow in the stator core in closed paths. They are called eddy currents or Foucault's currents. Finally, Lenz's law suggests that the current flows in a way so as to oppose the magnetic field producing it. Circulating eddy currents will face resistance and will dissipate energy

in the form of heat. Neglecting saturation, eddy current losses in sinusoidally excited material are given by $P_e = k_2 V f^2 \tau^2 \hat{B}^2$ [8], where k_2 is a constant of proportionality dependent on characteristics of iron and units used, V is the volume of iron, f is the frequency, τ is the lamination thickness, and $\hat{B}$ is peak flux density. We can infer that $P_e \propto \omega^2(\lambda_d^2 + \lambda_q^2)$ where ω is rotor speed, and λ_d and λ_q are flux components as described in Appendix A [4]. Therefore the equation describing eddy current losses in our motor will be given by

$$P_e = k_e \omega^2 (\lambda_d^2 + \lambda_q^2) \tag{9}$$

where k_e is a constant of proportionality dependent on characteristics of iron and units used, volume of iron, and lamination thickness. However Parker's catalog claims to have practically eliminated eddy current losses by using ultra thin lamination in their motor design [6].

Hysteresis Losses Cyclic energy conversion from one form to another and back to original form does not give the same amount of energy but less; i.e., some amount of energy is dissipated or lost as heat. In an electric motor, the changing magnetic field interacts with stator core which is iron. Iron is a ferromagnetic material i.e. whenever magnetic field is applied it will get magnetized. But when the field is removed it retains some of its magnetism. When the magnetic field reverses, extra work has to be done to overcome the retained magnetism. Hence we need to account for hysteresis losses in our model. The empirical equation that describes hysteresis losses is given by $P_h = k_3 V f \hat{B}^n$ [8], where k_3 is a constant of proportionality dependent on characteristics of iron and units used; V is the volume of iron; f is the frequency; n is the exponent, usually its value is 2; and $\hat{B}$ is peak flux density. We can infer that $P_h \propto \omega(\lambda_d^2 + \lambda_q^2)$. Therefore the equation describing hysteresis losses in our motor

will be given by

$$P_h = k_h \omega (\lambda_d^2 + \lambda_q^2) \tag{10}$$

where k_h is a constant of proportionality dependent on characteristics of iron and units used, and volume of iron.

3.2.1.3 Friction Losses

In permanent magnet synchronous motors, mechanical losses are due primarily to viscous friction and are proportional to ω^2 [8]. Therefore they can be modeled by

$$P_f = k_f \omega^2 \tag{11}$$

where k_f is the constant of proportionality known as the viscous friction coefficient.

3.2.2 Loss Model Validation

We can model total power losses P_t in the permanent magnet synchronous motor by

$$P_t = R(\theta_{m1})(i_d^2 + i_q^2) + k_e \omega^2 (\lambda_d^2 + \lambda_q^2) + k_h \omega (\lambda_d^2 + \lambda_q^2) + k_f \omega^2 \tag{12}$$

but we need to compute all constants of proportionality.

The datasheet [7] indicates that the phase resistance at 25 °C is $R_{25} = 0.009255$ ohms. In operation, the phase resistance will be larger due to an increase in temperature. For example, winding temperature under rated conditions is 140 °C and the corresponding phase resistance may be computed to be $R_{140} = 0.0134$ ohms using

$$R(\theta_1) = R(\theta_0)(1 + \alpha(\theta_1 - \theta_0)) \tag{13}$$

where α is the temperature coefficient of resistance of copper.

The datasheet also provides data for moving losses with no current flow. In general, such losses would consist of eddy current losses, hysteresis losses and friction losses, where the flux that determines iron loss is permanent magnet flux only.

Datasheet values for moving loss and speed result in following constraint equations on the coefficients of proportionality:

$$\begin{bmatrix} P_1 \\ \vdots \\ P_n \end{bmatrix} = \begin{bmatrix} \omega_1^2(\lambda_{d,1}^2 + \lambda_{q,1}^2) & \omega_1(\lambda_{d,1}^2 + \lambda_{q,1}^2) & \omega_1^2 \\ \vdots & \vdots & \vdots \\ \omega_n^2(\lambda_{d,n}^2 + \lambda_{q,n}^2) & \omega_n(\lambda_{d,n}^2 + \lambda_{q,n}^2) & \omega_n^2 \end{bmatrix} \begin{bmatrix} k_e \\ k_h \\ k_f \end{bmatrix}$$

This is a non-negative linear least squares problem, since all constants of proportionality are known to be non-negative from physics. The solution to this problem is

$$k_e = 0 \text{ W·s}^2\text{·rad}^{-2}\text{·Wb}^{-2}$$

$$k_h = 27.453 \text{ W·s·rad}^{-1}\text{·Wb}^{-2}$$

$$k_f = 0.0024 \text{ Nm·s·rad}^{-1}$$

where the zero value of k_e is consistent with Parker's claim to have practically eliminated eddy currents, and the value of k_f is consistent with the value of viscous friction coefficient mentioned in [7]. RMSE for the proposed moving loss model is 13.48 W, indicating a good fit. Figure 6 shows the modeled moving losses.

3.3 Thermal Modeling

3.3.1 Proposed Model with Network Topology

A simplified sketch of the cross section of our motor is shown in Figure 7. Black arrows indicate the direction of heat flow by conduction from winding to the stator core and from the stator core to the cooling jacket. The isothermal surfaces of significant interest to us are the winding at a temperature θ_{m1} and the stator core at a temperature θ_{m2} because these are the major contributors of losses in a permanent magnet synchronous motor. We do not consider the rotor as a node of interest because our motor uses Samarium Cobalt as permanent magnet, which has a Curie temperature of around $700 - 800$ °C. Therefore modeling of rotor temperature variation is unnecessary.

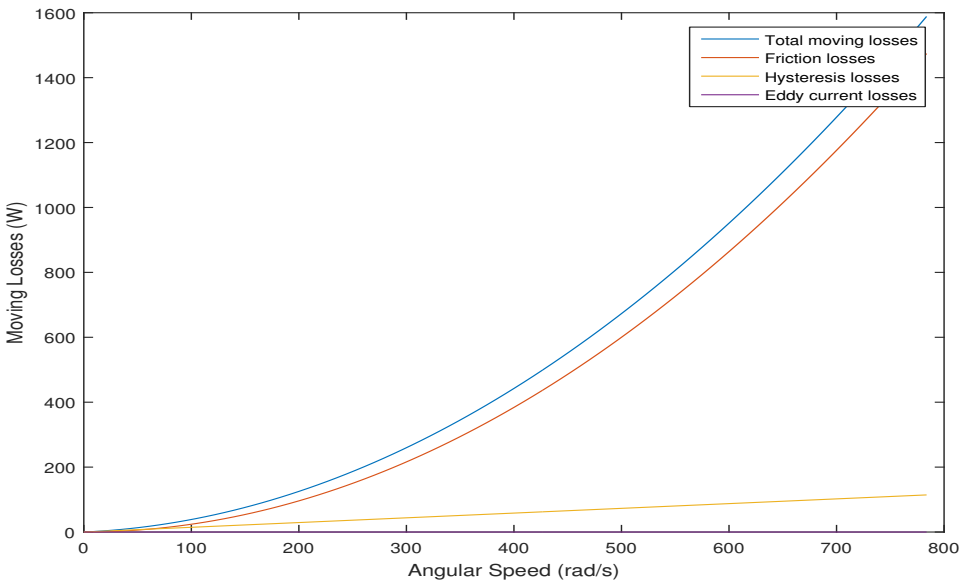

Figure 6: Motor moving losses.

Thermal resistance R_{m1} will lump the infinite possible heat flow paths between the winding and the stator core, similarly R_{m2} will lump the heat flow paths between stator core and cooling jacket. Since the winding and stator core have significant thermal mass and both contribute to losses, they will be associated with a thermal capacitor C_{m1} and C_{m2} respectively, and ideal independent heat flow sources P_1 and P_2 respectively. The third isothermal surface (node) will be the cooling jacket, which is assumed to be at a constant temperature with time and this node will be connected

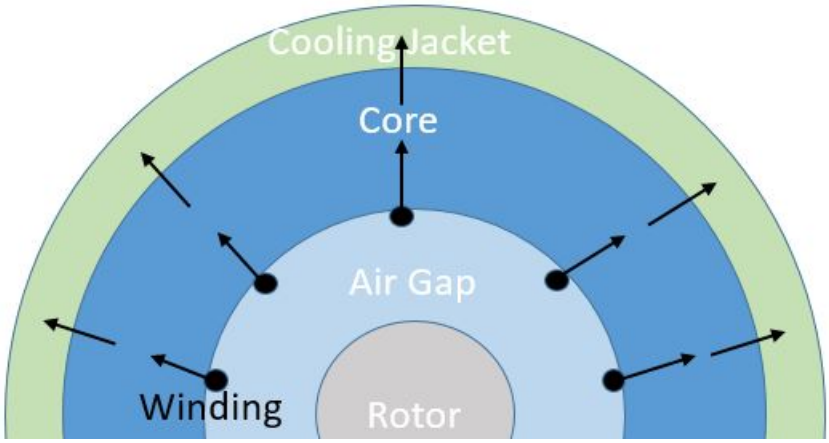

Figure 7: A sketch of heat flow in the motor.

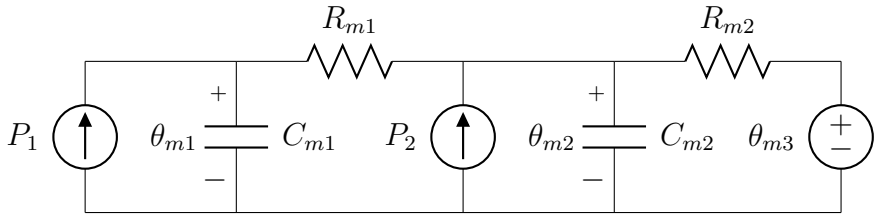

Figure 8: Proposed motor thermal network.

to an ideal independent temperature source θ_{m3}. These observations and inferences result in the thermal network shown in Figure 8. The state space model describing the thermal network in Figure 8 is given by (14)

$$\begin{bmatrix} \dot{\theta}_{m1} \\ \dot{\theta}_{m2} \end{bmatrix} = \begin{bmatrix} \frac{-1}{R_{m1}C_{m1}} & \frac{1}{R_{m1}C_{m1}} \\ \frac{1}{R_{m1}C_{m2}} & -(\frac{1}{R_{m1}C_{m2}} + \frac{1}{R_{m2}C_{m2}}) \end{bmatrix} \begin{bmatrix} \theta_{m1} \\ \theta_{m2} \end{bmatrix} + \begin{bmatrix} \frac{1}{C_{m1}} & 0 \\ 0 & \frac{1}{C_{m2}} \end{bmatrix} \begin{bmatrix} P_1 \\ P_2 \end{bmatrix} + \begin{bmatrix} 0 \\ \frac{\theta_{m3}}{R_{m2}C_{m2}} \end{bmatrix} \tag{14}$$

where P_1 represents the copper losses, θ_{m1} represents the copper winding temperature, P_2 represents the combination of iron losses and friction losses, θ_{m2} represents temperature of the stator iron and θ_{m3} represents temperature of the coolant. For simplicity in computing thermal model parameters, we assume that copper losses do not change with temperature.

3.3.2 Thermal Model Parameters

3.3.2.1 Thermal Resistance

At steady state, the network in Figure 8 reduces to the network in Figure 9. The Parker datasheet provides the thermal resistance between winding and coolant i.e.

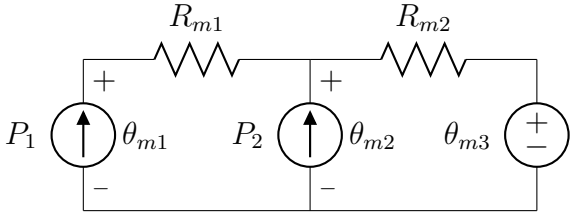

Figure 9: Motor thermal network at steady state.

$R_{m1} + R_{m2} = 0.052$ °C/W, and also provides the thermal resistance between winding and core i.e. $R_{m1} = 0.037$ °C/W [7]. We can compute R_{m2} by applying principle of superposition. The computed value of R_{m2} is 0.015 °C/W.

3.3.2.2 Thermal Capacitance

The proposed thermal network is linear time invariant. We can capitalize on this fact and use the definition of eigenvalues for computing the thermal capacitances. The datasheet provides two time constants. Copper winding time constant τ_1 and stator core time constant τ_2 are given as:

$$\tau_1 = 150 \text{ s}$$

$$\tau_2 = 606 \text{ s}$$

The eigenvalues will be real and negative:

$$\lambda_1 = \frac{-1}{\tau_1}$$
$$\lambda_2 = \frac{-1}{\tau_2}$$

Solving for the eigenvalues of A matrix in (14) by $|\lambda I - A| = 0$ gives a quadratic equation in λ with the sum of the roots given by

$$\frac{1}{R_{m1}C_{m2}} + \frac{1}{R_{m2}C_{m2}} + \frac{1}{R_{m1}C_{m1}} = -\lambda_1 - \lambda_2 \tag{15}$$

and product of the roots given by

$$\frac{1}{R_{m1}R_{m2}C_{m1}C_{m2}} = \lambda_1\lambda_2 \tag{16}$$

Solving (15) and (16) simultaneously generates

$$C_{m1} = 4903.6 \text{ J/°C}$$

$$C_{m2} = 33401 \text{ J/°C}$$

3.3.3 Thermal Model Validation

The motor rated torque at zero speed is 146.56 Nm; the peak torque at zero speed is 256.82 Nm. The proposed model was coded in MATLAB and simulated for 5000 s at rated condition to produce a steady-state winding temperature of 140 °C. Since we do not know how Parker computed i_d and i_q to generate their data, we provide a reasonable strategy in Appendix A in order to obtain the heat flow sources as previously modeled. The results reported in Table 2 exhibit small errors that may be due to differences between assumed and implemented excitation strategy.

Table 2: Winding Temperature at Rated Condition

Torque (Nm)	Speed (rad/s)	Computed Winding Temperature (°C)	Percent Error
146.37	34.83	137.9	-1.5
144.71	182.87	137.7	-1.64
143.26	261.24	137.7	-1.64
139.35	409.27	137.7	-1.64
121.05	548.6	140.1	0.071
84.5	714.06	139.6	-0.28

CHAPTER IV

INVERTER THERMAL MODELING

4.1 Introduction

We have purchased SEVCON's Gen4 Size8 water cooled inverter. The main function of the inverter is to control power to the permanent magnet synchronous motor present in our hybrid electric vehicle. The Gen4 Size8 employs a 6 switch IGBT bridge consisting of 6 transistors and 6 anti-parallel diodes. The inverter is designed with minimum thermal resistances and with an ability to protect itself if temperatures are excessive. As end users of this product, we must understand the duration for which we can push the inverter to its limits without exceeding the temperature constraints.

Intrinsic temperature of a semiconductor is the temperature above which rectification functionality of IGBT switches is lost; i.e., the p-n junction is shorted out [5]. SEVCON has not provided us with the intrinsic temperature but they have given the maximum IGBT junction temperature. From experience it is less than the intrinsic temperature of an IGBT. Above the maximum IGBT junction temperature, reliability of the product is not guaranteed by the manufacturer. Hence, it is our responsibility to develop a thermal model of the inverter to ensure its proper use.

4.2 Loss Modeling

Losses determine heating of the inverter. The principal sources of heat will be switching losses, conduction losses and quiescent losses. These are discussed in detail below.

4.2.1 Dissipation Mechanisms

4.2.1.1 Switching Losses

Heat is dissipated in the power semiconductors during the turn on interval, t_{on}, and the turn off interval, t_{off}. Given the switching frequency, f_s, the switching power loss can be approximated by $\frac{1}{2}V_{dc}I_{rms}f_s(t_{on}+t_{off})$ [5]. Rewriting the equation we get

$$P_s = k_s V_{dc} I_{rms} \tag{17}$$

where k_s is a proportionality constant dependent on t_{on}, t_{off} and f_s. The notation V_{dc} and I_{rms} are clarified in Appendix A.

4.2.1.2 Conduction Losses

During operation, inverter leg currents pass through either power transistors or power diodes. Transistor conduction losses can be approximated with on state zero current collector emitter voltage and collector emitter on state resistance. Similarly, diode conduction losses can be approximated by a forward voltage drop and an on state resistance. Therefore, we can model the conduction losses by

$$P_c = k_{c1} I_{rms} + k_{c2} I_{rms}^2 \tag{18}$$

where k_{c1} is dependent on the transistor's on state zero current collector emitter voltage and the diode's forward voltage drop, while k_{c2} depends on the on state resistances of the transistor and its anti-parallel diode.

4.2.1.3 Quiescent Losses

The inverter draws power under no load and no switching but enabled condition. These losses are the quiescent power losses and are given by

$$P_q = k_o \tag{19}$$

where k_o is the quiescent power consumption of the inverter.

4.2.2 Loss Model Validation

We can model total power loss P in the inverter by

$$P = k_o + k_s V_{dc} I_{rms} + k_{c1} I_{rms} + k_{c2} I_{rms}^2 \tag{20}$$

but we need to compute all constants of proportionality.

The SEVCON Gen4 Size8 application note provides losses at various currents for a bus voltage of 175 V and 300 V [10]; our application uses a bus voltage of 350 V. These values result in the following constraint equations on the coefficients of proportionality:

$$\begin{bmatrix} P_1 \\ \vdots \\ P_n \end{bmatrix} = \begin{bmatrix} 1 & V_{dc} I_{rms,1} & I_{rms,1} & I_{rms,1}^2 \\ \vdots & \vdots & \vdots & \vdots \\ 1 & V_{dc} I_{rms,n} & I_{rms,n} & I_{rms,n}^2 \end{bmatrix} \begin{bmatrix} k_o \\ k_s \\ k_{c1} \\ k_{c2} \end{bmatrix}$$

This is a non-negative linear least squares problem, since all constants of proportionality are known to be non-negative from physics. The solution to this problem is

$$k_o = 29.7208 \text{ W}$$

$$k_s = 0.013$$

$$k_{c1} = 1.7095 \text{ V}$$

$$k_{c2} = 0.0147 \text{ ohms}$$

RMSE for the proposed inverter power loss model is 10.17 W, indicating a good fit. Figure 10 shows the modeled inverter power losses at a bus voltage of 350 Vdc, 300 Vdc and 175 Vdc.

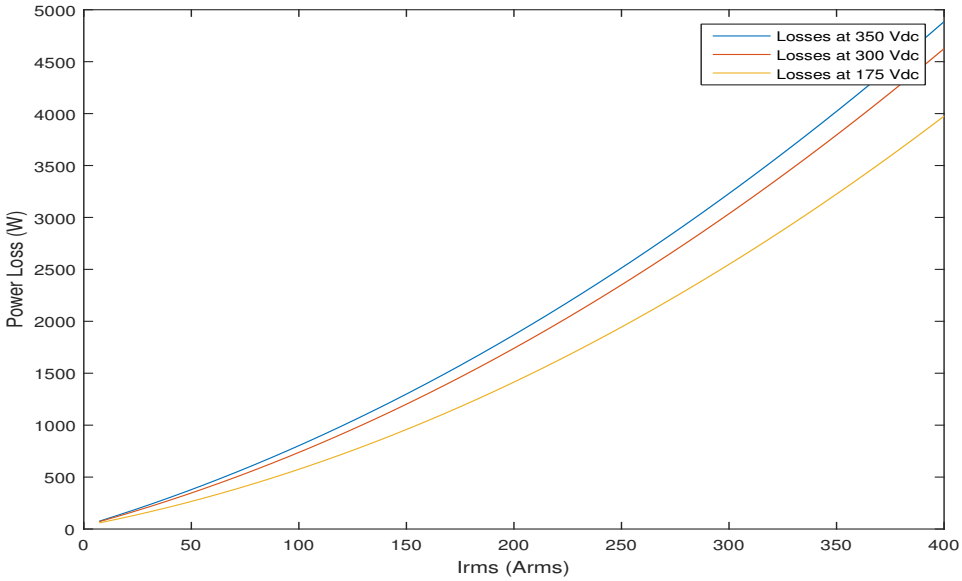

Figure 10: Inverter losses at 350 Vdc.

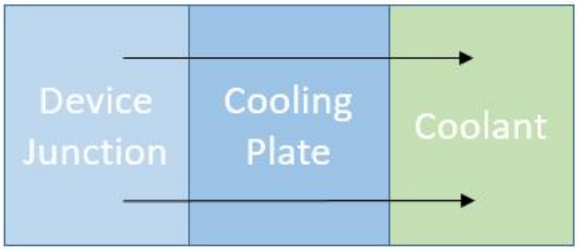

Figure 11: A sketch of heat flow in the inverter.

4.3 Thermal Modeling

4.3.1 Proposed Model with Network Topology

A simplified sketch of the inverter is shown in Figure 11. The black arrows indicate the flow of heat from the device junction to the coolant via the cooling plate. The isothermal surfaces of interest to us are the device junction at temperature θ_{i1}, the cooling plate at temperature θ_{i2}, and the coolant at temperature θ_{i3}. We assume negligible thermal mass of the power transistor and its anti-parallel diode. The only significant contribution to the thermal mass is made by the cooling plate, therefore, the cooling plate is associated with a thermal capacitor C_i. Since the only source of

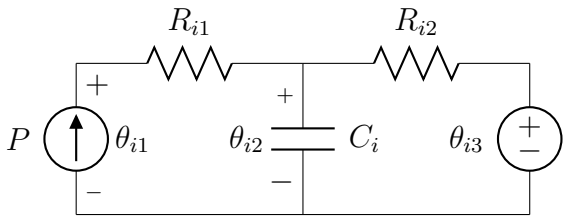

Figure 12: Proposed inverter thermal network.

loss is the power transistor and its anti-parallel diode, we associate an ideal independent heat flow source with the device junction node. The third node, which is the coolant, is assumed to be at a constant inlet temperature, therefore, it is connected to an ideal independent temperature source. A thermal resistance R_{i1} will lump the heat flow paths between the device junction and the cooling plate, while thermal resistance R_{i2} will lump the heat flow paths between the cooling plate and the coolant. These observations, assumptions and inferences result in the thermal network in Figure 12. Equation (21) describes the proposed inverter thermal model

$$\dot{\theta}_{i2} = \frac{R_{i2}P - \theta_{i2} + \theta_{i3}}{C_i R_{i2}} \tag{21}$$

where P is the sum of switching losses, conduction losses and quiescent losses.

4.3.2 Thermal Model Parameters

4.3.2.1 Thermal Resistance

At steady state the proposed inverter thermal network reduces to the network in Figure 13. The SEVCON application note gives the value of R_{i2} at a flow rate of 2.5 lpm. In the context of the steady state thermal network, the operating condition described by the current flow of 257 Arms, and bus voltage of 300 Vdc, results in the variables assuming the values of

$$\theta_{i1} = 145 \text{ °C}$$

$$P = 2448.1 \text{ W}$$

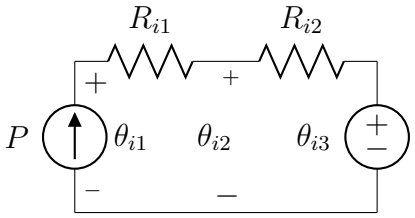

Figure 13: Inverter thermal network at steady state.

while the constants in the steady state thermal network have the values of

$$\theta_{i3} = 65\ ^{\circ}\text{C}$$

$$R_{i2} = 0.0186\ ^{\circ}\text{C/W}$$

From the available information we can compute θ_{i2} by:

$$\theta_{i2} = R_{i2}P + \theta_{i3} = 110.53\ ^{\circ}\text{C}$$

Finally, R_{i1} can be calculated by:

$$R_{i1} = \frac{\theta_{i1} - \theta_{i2}}{P} = 0.014\ ^{\circ}\text{C/W}$$

4.3.2.2 Thermal Capacitance

The SEVCON Gen4 Size8 application note specifies that the inverter can be operated at a current flow of 300 Arms, bus voltage of 300 Vdc and a flow rate of 2.5 lpm for 120 s. This implies that at 120 s, the device junction temperature will be $\theta_{i1} = 145\ ^{\circ}\text{C}$. The power loss in the inverter at 300 Vdc and 300 Arms will be $P = 3038.3$ W. With this knowledge, we can calculate thermal capacitance C_i from (22):

$$\theta_{i1} = R_{i1}P + \theta_{i3} + R_{i2}P(1 - e^{\frac{-t}{R_{i2}C_i}}) \tag{22}$$

The computed value of thermal capacitance is $C_i = 5935.2$ J/°C. The cooling plate arrangement is made of aluminum. Aluminum has a specific heat capacity of 900 J/kgK. We can compute the mass of the cooling plate using the relation $m = \frac{C_i}{c_p} = 6.6$ kg, which is less than the mass of the inverter 10 kg. This is a simple reality check.

Table 3: Model Predicted Junction Temperature at 300 Vdc

Current (Arms)	Simulation Time (s)	Computed Junction Temperature (°C)	Percent Error
190	3000	118	-
257	3000	144.61	-0.27
300	120	144.84	-0.11
400	10	136.53	-5.8

Table 4: Model Predicted Junction Temperature at 175 Vdc

Current (Arms)	Simulation Time (s)	Computed Junction Temperature (°C)	Percent Error
220	3000	117.74	-
292	3000	144.75	-0.17
300	200	140.31	-3.23
400	45	145.05	0.03

4.3.3 Thermal Model Validation

The proposed model was coded in MATLAB and simulated for the time constraints mentioned in the application note. Table 3 and Table 4 show computed junction temperature for a bus voltage of 300 Vdc and 175 Vdc respectively. We were able to develop a reasonable inverter thermal model given the limited data from the manufacturer.

CHAPTER V

CONCLUSION

In this thesis we not only explained the basics of heat transfer, thermal modeling and losses, but also applied these concepts to develop thermal model for the permanent magnet synchronous motor and the inverter. We estimated the power losses in the motor and the inverter, and fed them into the thermal models to simulate average temperature rises of critical components.

5.1 General Conclusions

1. Motor and inverter thermal models provide an effective and efficient way to estimate average temperature rises via simulations. They can aid the selection process of a motor and an inverter, and form an integral part of on line temperature estimation scheme.

2. The procedure developed to model the motor power losses and the inverter power losses is simple yet generic. The power loss models are completely scalable.

3. The motor and inverter thermal model will vary according to the purpose and objective of the designer. However, the procedure used to develop the lumped parameter thermal models is standard and effective.

5.2 Specific Conclusions

1. GVM 210-150P uses Samarium Cobalt based permanent magnets. If the magnets were not made of high temperature rare earth based materials, then it would have been imperative to simulate rotor temperature rise.

2. We are confident that at rated conditions the motor can be operated indefinitely, but it would be interesting to know if the inverter limits the motor operation at rated condition or not. Secondly, we could also figure out whether the inverter or the motor limits the ensemble level operation at higher torques. For the interpretations to make sense, it is necessary to mention the operating conditions. The motor operating conditions are: bus voltage of 350 Vdc, coolant flow rate of 5 lpm and coolant temperature of 60 °C; the inverter operating conditions are: bus voltage of 350 Vdc, coolant flow rate of 2.5 lpm and coolant temperature of 65 °C. Table 5 shows the time to reach critical temperature in the motor and the inverter at various torque and speed values. As we increase the requested torque to values closer to the peak torque, we can observe that the inverter is the limiting component. We would also like to remind that the strategy described in Appendix A to select motor currents does not account for magnetic saturation, hence, at torque values closer to the peak torque, the time required to reach critical winding temperature would occur earlier than predicted.

3. The SEVCON application note mentions that the long term rating of the inverter will be limited by DC link capacitor temperature. Therefore, we can conclude that at an ensemble level, the inverter will be a limiting component in our application.

4. Our team has decided to operate the inverter at a coolant flow rate of 5 lpm. Therefore, we could expect a better performance from the inverter than reported in Table 5.

5.3 Recommendations for Further Research

Next logical step in this direction would be to improve the inverter thermal model; i.e., collect more useful data and compute thermal resistance of the cooling plate

Table 5: Time to Reach Critical Temperatures

Torque (Nm)	Speed (rad/s)	Current (Arms)	Time to critical junction temperature(°C)	Time to critical winding temperature(°C)
146.37	34.83	193.2	Indefinite	Indefinite
121.05	548.6	180.5	Indefinite	Indefinite
200	300	264	200	278
255.83	200.28	337	53	130

of the inverter at 5 lpm. The motor and inverter thermal model can be integrated in a Simscape based motor torque control simulation to adjust requested torque in response to temperature rise. Also these models can be part of an on line temperature estimation scheme.

APPENDIX A

SOME THEORETICAL RESULTS

A.1 Voltage Limits

Our motor is WYE connected. Assume converter leg voltages v_A, v_B and v_C. Given the source imposed physical limitations on converter leg voltages:

$$0 \leq v_A \leq V_{dc}$$

$$0 \leq v_B \leq V_{dc}$$

$$0 \leq v_C \leq V_{dc}$$

The maximum length of the dq voltage vector is given by [9]:

$$V_{max} = \sqrt{\frac{3}{8}} V_{dc}$$

where V_{dc} is the bus voltage of the inverter. This result is derived assuming sine triangle modulation, however, SEVCON uses space vector modulation which results in a more favorable bus voltage utilization.

A.2 Current Limits

Assume converter leg currents i_A, i_B and i_C. Given the physical limitations on converter leg currents due to the maximum allowable current permitted to flow through the switches

$$|i_A| \leq I_{leg,max}$$

$$|i_B| \leq I_{leg,max}$$

$$|i_C| \leq I_{leg,max}$$

where $I_{leg,max}$ is the maximum leg current. The maximum length of the dq current vector is given by [9]:

$$I_{max} = \sqrt{\frac{3}{2}} I_{leg,max}$$

A.3 Torque Control

If a requested torque is strictly less than the capability limit at the given speed, then there will be an infinite number of current vectors that achieve the requested torque. Therefore, a rule for selecting dq current components must be established. Here the focus will be on minimizing copper losses, and the rule is sometimes referred to as MTPA or maximum torque per amp [9].

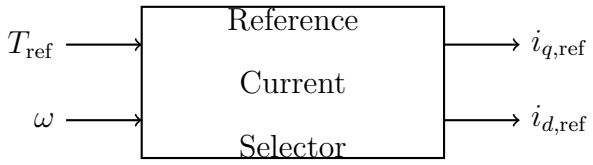

Since torque depends on q-axis current but not d-axis current, the rule for selecting an appropriate reference value for q-axis current is straightforward:

$$i_{q,\text{ref}} = \frac{T_{\text{ref}}}{\Lambda N}.$$

where $\Lambda = \sqrt{\frac{3}{2}}\Lambda_m$ and Λ_m is the maximum value of permanent magnet flux, and N is number of pole pairs. The rule for selecting an appropriate reference value for d-axis current involves two cases, low-speed operation where flux weakening is not needed, and high-speed operation where flux weakening is needed. These two cases are expressed by

$$i_{d,\text{ref}} = \begin{cases} 0 & , \ \omega \leq \omega_{0,\text{ref}} \\ -\dfrac{\Lambda}{L} + \sqrt{\left(\dfrac{V_{\max}}{N\omega L}\right)^2 - i_{q,\text{ref}}^2} & , \ \text{otherwise} \end{cases}$$

where L is the effective inductance, and $\omega_{0,\text{ref}}$ is given by

$$\omega_{0,\text{ref}} = \frac{V_{\max}}{N\sqrt{\Lambda^2 + L^2 i_{q,\text{ref}}^2}}.$$

The threshold speed $\omega_{0,\text{ref}}$ is defined such that continuity is imposed at $i_{d,\text{ref}} = 0$.

A.4 RMS Inverter Leg Current

We have used MTPA to compute motor currents i_d and i_q. The rms value of current through an inverter leg will be given by [9]:

$$I_{rms} = \frac{\sqrt{i_d^2 + i_q^2}}{\sqrt{3}}$$

APPENDIX B

LISTINGS OF MATLAB PROGRAMS

B.1 Code for Motor Thermal Model

```
% Motor Thermal Model
% User Inputs: Torque(Tref) and Speed(wref)
% Inputs for scalability: Battery Voltage(Vdc) and Initial Temperatures
% For motor operation both below and above base speed
% Outputs: Winding Temperature and Case Temperature

clc
close all
clear all

%% Motor and Inverter Electrical Parameters
R=0.009255;   % Winding resistance in ohms
L=1.37*10^-4;  % Winding inductance in henry
lambda=0.0729; % Permanent mgnet flux linkage in V/rad/s
N=6;           % Pole pairs
Vdc=350;       % Nominal battery voltage
ILegMax=400*sqrt(2);   % Maximum current allowed through inverter leg

%% Motor Thermal Network Parameters
% Thermal Resistances (Rth) in degree C/W
R1=0.037;      %Rth between winding and case
R2=0.015;      %Rth between case and coolant
% Thermal Capacitances (Cth) in J/degree K
C1=4903.6;     %Cth of winding
C2=33401;      %Cth of case
```

```
% Heat Sources in W
P1=0;           %initalized Copper Losses
P2=0;           %initalized Moving Losses

%% Enter the torque @ motor shaft (Nm) and rotor speed (rad/s)
Tref=input('Enter the torque in N-m : ');
wref=input('Enter the speed of the rotor shaft in rad/s : ');

tic
%% Compute id and iq using Maximum Torque Per Ampere (MTPA)
Vmax=sqrt(3/8)*Vdc;
Imax=sqrt(3/2)*ILegMax;
% q axis reference currents
Iqref=Tref/(N*lambda);
% Influence of current limits
if (Iqref^2<Imax^2)
   disp('Currents computed are valid')
end
% Influence of voltage limit
wmaxref=Vmax/(N*L*Iqref);
% Onset of flux weakening
w0ref=Vmax/(N*sqrt(lambda^2+L^2*Iqref^2));
% d axis reference currents
if (wref < w0ref)
    Idref=0;
else
    Idref=(-lambda/L)+sqrt((Vmax/(N*wref*L))^2-Iqref^2);
end

%% Thermal model
% Initializing temperature varaibles
theta3=60;        % Maximum coolant inlet temperature in degree C
```

```
theta1(1)=theta3; % Initial winding temperature
theta2(1)=theta3; % Initial case temperature
% The 2 node system
h=1;                % Step size in seconds
t=3000;             % Total simulation time
% Losses
ke=0;                % Eddy losses constant of proportionality
kh=27.453;           % Hysteresis losses constant of proportionality
kf=0.0024;           % Friction losses constant of proportionality
P2=ke*(wref^2*((L*Idref+lambda)^2+(L*Iqref)^2))+kh*wref*((L*Idref+lambda
    )^2+(L*Iqref)^2)+kf*wref^2;
% Euler iterations
for i=1:1:t
    P1=R*(1+3.93*10^-3*(theta1(i)-25))*(Idref^2+Iqref^2); %copper losses
    w_slope(i)=(P1/C1)-(theta1(i)/(C1*R1))+(theta2(i)/(C1*R1));
    theta1(i+1)=theta1(i)+h*(w_slope(i));

    c_slope(i)=(P2/C2)+(theta1(i)/(C2*R1))-(theta2(i)/(C2*R1))-(theta2(i
    )/(C2*R2))+(theta3/(C2*R2));
    theta2(i+1)=theta2(i)+h*(c_slope(i));

end

toc

figure(1)
plot(1:t,theta2(1:t))
title('Aggregated case temperature')
xlabel('time in seconds')
ylabel('Temperature in degree C')
figure(2)
plot(1:t,theta1(1:t))
```

```
title('Aggregated winding temperature')
xlabel('time in seconds')
ylabel('Temperature in degree C')
```

B.2 Code for Inverter Thermal Model

```
% Inverter Thermal Model
% User Inputs: Torque(Tref) and Speed(wref)
% Inputs for scalability: Battery Voltage(Vdc) and Initial Temperatures
% For motor operation both below and above base speed
% Outputs: Junction Temperature and Cooling plate Temperature

clc
clear all
close all

%% Motor and Inverter Electrical Parameters
Rs=0.009255;   % Winding resistance in ohms
L=1.37*10^-4;  % Winding inductance in henry
lambda=0.0729; % Permanent mgnet flux linkage in V/rad/s
N=6;           % Pole pairs
Vdc=350;       % Nominal battery voltage
ILegMax=400*sqrt(2);   % Maximum current allowed through inverter leg

% Inverter Thermal Network Parameter
%Thermal Resistances (Rth) in degree C/W
R1=0.014;      %Rth between junction and heatsink/baseplate
R2=0.0186;     %Rth between heatsink/baseplate and cooling jacket
%Thermal Capacitances (Cth) in J/degree K
C1=5935.2;   %Cth of baseplate/heatsink
%Heat Sources in W
P1=0;          %Losses in IGBTs

%% Enter the torque @ shaft (N-m) and rotor speed (rad/s)
```

```
Tref=input('Enter the torque in N-m : ');
wref=input('Enter the speed of the rotor shaft in rad/s : ');

tic
%% Compute id and iq using Maximum Torque Per Ampere (MTPA)
Vmax=sqrt(3/8)*Vdc;
Imax=sqrt(3/2)*ILegMax;
% q axis reference currents
Iqref=Tref/(N*lambda);
% Influence of current limits
if (Iqref^2<Imax^2)
   disp('Currents computed are valid')
end
% Influence of voltage limit
wmaxref=Vmax/(N*L*Iqref);
% Onset of flux weakening
w0ref=Vmax/(N*sqrt(lambda^2+L^2*Iqref^2));
% d axis reference currents
if (wref < w0ref)
    Idref=0;
else
    Idref=(-lambda/L)+sqrt((Vmax/(N*wref*L))^2-Iqref^2);
end

% Thermal Model
%Initializing temperature varaibles
theta3=65;      % Maximum coolant inlet temperature in degree C
theta2(1)=65;  % initial heat sink temperature
theta1=65;      % initial junction temperature
%The 2 node system
h=1;            % Step size in seconds
t=3000;         % Total simulation time
```

```
%IGBT losses
ko=29.7208;
ks=0.013;
kc1=1.7095;
kc2=0.0147;
Ieff=sqrt((Idref^2+Iqref^2)/3);
P1=ko+ks*Vdc*Ieff+kc1*Ieff+kc2*Ieff^2;
%Euler iterations
for i=1:1:t
    h_slope(i)=(P1/C1)-(theta2(i)-theta3)/(R2*C1);
    theta2(i+1)=theta2(i)+h*(h_slope(i));
end

toc

theta1=R1*P1+theta2(i);
figure(1)
plot(1:t,theta2(1:t))
title('Aggregated heatsink plus baseplate temperature')
xlabel('time in seconds')
ylabel('Temperature in degree C')
```

REFERENCES

[1] Bergman, T. L., Lavine, A. S., Incropera, F. P., and Dewitt, D. P., *Fundamentals of Heat and Mass Transfer*. John Wiley and Sons, 2011.

[2] Cox, D. and Sriram, G., "Georgia tech vehicle design report," tech. rep., Georgia Institute of Technology, Atlanta, Georgia, Dec. 2015.

[3] Dorny, N. C., *Understanding Dynamic Systems: Approaches to Modeling, Analysis and Design*. Prentice Hall, 1993.

[4] Milanfar, P. and Lang, J., "Monitoring the thermal condition of permanent magnet synchronous motors," IEEE Trans. Aerosp. Electron. Syst., Oct 1996.

[5] Mohan, N., Undeland, T. M., and Robbins, W. P., *Power Electronics: Converters, Applications, and Design*. Wiley, 2011.

[6] Parker Hannafin Corporation, *GVM Motor Solutions*, July 2014.

[7] Parker Hannafin Corporation, *GVM210-150P6 Datasheet*, Oct. 2015.

[8] Sarma, M., *Electric Machines: Steady-State Theory and Dynamic Performance*. West Publishing Company, 1994.

[9] Taylor, D., "Control system design: 4550 course notes." Handed out by advisor, Oct. 2014.

[10] Taylor, R., *Gen4 Application Note*. SEVCON, April 2013.

[11] Venkatraman, B., Godsey, B., Premerlani, W., Shulman, E., Thakur, M., and Midencce, R., "Fundamentals of a motor thermal model and its application in motor protection," IEEE 58th Annual Conference for Protective Relay Engineers, April 2005.